BioEnergy Research (2019) 12:275–291
https://doi.org/10.1007/s12155-019-09967-8

A Comparison of Ionic Liquids and Organic Solvents on the Separation of Cellulose-Rich Material from River Red Gum

Pobitra Halder[1] · Sazal Kundu[1] · Savankumar Patel[1] · Mohammad Ramezani[1] · Rajarathinam Parthasarathy[1] · Kalpit Shah[1]

Published online: 12 April 2019

Abstract

With the aim of separating cellulose-rich material from river red gum, it was pre-treated with three ionic liquids (ILs), i.e. 1-butyl-3-methylimidazolium chloride ([Bmim][Cl]), 1-ethyl-3-methylimidazolium acetate ([Emim][OAc]) and 1-butyl-3-methylimidazolium acetate ([Bmim][OAc]) as well as with two organic solvents, i.e. methanol and ethanol. All ILs and organic solvents were able to remove more than 20% lignin. The [Emim][OAc] was found to be the most effective IL in removing lignin (i.e. 26.2 wt% lignin was removed) amongst all pre-treatment studies. Noticeable structural differences were observed in the cellulose-rich materials obtained from IL and organic solvent pre-treatments and several analytical instruments such as XRD, FTIR, TGA and SEM were employed for their detailed understandings. ILs, in contrast to organic solvents, produced porous and low crystalline cellulose-rich material. This was believed to be due to the transformation of crystalline cellulose I to amorphous cellulose II during IL pre-treatment. The exciting findings of producing high porosity and low crystallinity cellulose-rich material along with the removal of lignin using IL treatment have the potential to transform the future bio-processing and bio-refining industry. More than 80% IL recovery was achieved in this investigation. A minor structural alteration was observed in the recovered [Bmim][Cl] while no structural change was observed in the recovered [Emim][OAc] and [Bmim][OAc], and this was confirmed by FTIR spectroscopic analyses. This establishes the recyclability and reusability of ILs in the cost effective pre-treatment of biomass.

Keywords Delignification · River red gum · Ionic liquid pre-treatment · Organic solvent pre-treatment · Biofuels · Biochemicals

Introduction

The global demand of sustainable and environmentally friendly renewable energy is increasing significantly because of greenhouse gas emissions from fossil fuels and their associated impacts on the climate change [1]. Lignocellulosic biomass has the potential to play a key role in fulfilling the high energy demand due to its abundancy and the prospect of converting it into fuels and other value-added products. Lignocellulosic biomass consists of semicrystalline cellulose, amorphous hemicellulose and aromatic polymers of lignin [2]. It is estimated that Australia has the potential of generating approximately 80 million tonnes lignocellulosic biomass per year and this number is expected to increase up to 110–115 million tonnes per year in the next 20–40 years [3].

River red gum (*RRG*) (*Eucalyptus camaldulensis*), a species of eucalypt family, is one such example of woody lignocellulosic biomass. Eucalyptus is native to Australia and approximately three quarter of the Australian forest, equivalent to 92 million hectares, is eucalypt forest where majority trees are *RRG* [4]. In South Australia, almost 50% of the total annual firewood consumption (410,000 t) is met by *RRG* [4]. *RRG* can be considered as an energy crop as it requires low water and fertiliser for its growth. *RRG* biomass mainly comprises of cellulose (46–49%), hemicellulose (18–23%), lignin (29–33%), ash (0.1–0.2%) and extractives (2–5%) [5]. The major advantage of *RRG* is that it contains very low amount of ash and extractives compared to many other agricultural lignocellulosic wastes such as sugarcane bagasse [6]. Therefore, it is considered to be one of the most promising candidates for biofuel and biochemical production [7, 8]. It is

Electronic supplementary material The online version of this article (https://doi.org/10.1007/s12155-019-09967-8) contains supplementary material, which is available to authorized users.

✉ Kalpit Shah
kalpit.shah@rmit.edu.au

[1] Chemical & Environmental Engineering, School of Engineering, RMIT University, Melbourne, Victoria 3000, Australia

estimated that *RRG* tree planted in one hectare area has the potential to produce approximately 7000 l of bioethanol [9].

Recent research on lignocellulosic biomass treatment [10, 11] is focusing on separating lignin and cellulose-rich fractions and further processing them to produce value-added materials as highlighted in Fig. 1.

Several chemical pre-treatment methods such as dilute acid treatment, alkali treatment and organic solvent treatment have been reported in the literature for separating lignin- and cellulose-rich fractions [11]. In the case of organic solvent treatment, known as OrganoSolv pre-treatment, chemicals such as ethanol, methanol, ethylene glycol, glycerol, acetic acid and formic acid have been extensively studied with and without catalysts [12–14]. Among these organic solvents, low boiling point alcohols such as ethanol and methanol are considered to be the most favourable solvents for OrganoSolv pre-treatment due to their low cost [15]. However, there are several shortcomings reported for OrganoSolv pre-treatment in the literature such as low solvent recovery as well as environmental, health and safety hazards associated with the high volatile and flammability properties of organic solvents [15].

Recently, the IL-based pre-treatment of lignocellulosic biomass, known as IonoSolv pre-treatment, has gained notable interests [16–23]. IonoSolv pre-treatment can effectively extract lignin from lignocellulosic biomass. Additionally, acidic IL treatment of lignocellulosic biomass for the production of platform chemicals such as furfural, 5-hydroxymethylfurfural (5-HMF) and levulinic acid is also attractive to the scientific community. For instance, the direct hydrolysis of cellulose and hemicellulose fractions using acidic ILs is an attractive approach for platform chemical production [24–27]. ILs are low temperature organic salts and these organic salts have a wide range of benefits including negligible vapour pressure, non-flammability and chemical and thermal stability. In addition, their properties can be tuned by combining various anions and cations from a large range of selections, their recovery is easy as they are low vapour pressure compounds and they are environmentally sustainable [28, 29]. To date, a wide numbers of ILs have been synthesised from the combinations of trillions of cations and anions [30] and employed in the biomass dissolution study. Among the imidazolium based ILs, 1-butyl-3-methylimidazolium chloride ([Bmim][Cl]), 1-ethyl-3-methylimidazolium acetate ([Emim][OAc]) and 1-butyl-3-methylimidazolium acetate ([Bmim][OAc]) showed promising results on lignin separation from lignocellulosic structure [31–33].

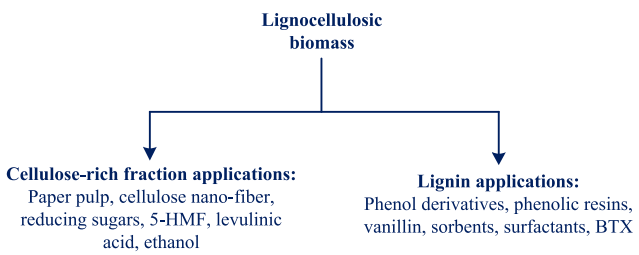

Fig. 1 Production of value-added materials from lignin and cellulose-rich fractions

While there are numerous studies focusing on various approaches of biomass pre-treatments, the studies published on IonoSolv pre-treatment for separating cellulose-rich fraction from biomass are still very limited when compared to OrganoSolv pre-treatment [31, 34–37]. Moreover, *RRG*, despite its huge potential in many parts of the world including Australia, has not been studied extensively with organic solvents and ILs for its pre-treatment. It is still unclear which pre-treatment method (i.e. OrganoSolv treatment or IonoSolv treatment) works better for recovering cellulose-rich fraction from *RRG*. It is yet not known which ILs can work better for the pre-treatment of *RRG* and how comparable those ILs will be with organic solvents. Additionally, morphological transformations observed in the cellulose-rich material obtained from IL and organic solvent pre-treatments are also not explored in detail. In this work, the IonoSolv pre-treatment of *RRG* is compared with the OrganoSolv pre-treatment of the same biomass on the basis of several measurable factors including the degree of delignification, morphological changes in the cellulose-rich material structure, thermal stability and cellulose crystallinity index (*CrI)*. The comprehensive study on both OrganoSolv and IonoSolv pre-treatments presented in this work discloses several interesting findings as reported further in the "Results and Discussion" sections.

Experimental

Materials

The biomass sample employed in this investigation was from *RRG* tree and it was sourced from a local Victorian supplier. The material was grinded and sieved to obtain particles in the range between 75 and 150 μm. The proximate and ultimate analyses of the untreated *RRG* were carried out using TGA Q500IR and LECO CHNS 932, and the results are tabulated in Table 1.

Before initiating any pre-treatment experiment, *RRG* was dried at 90 °C for 4 h. The ILs, employed in this investigation, are [Emim][OAc] (purity ≥ 95%), [Bmim][OAc] (purity ≥ 95%) and [Bmim][Cl] (purity ≥ 98%). These ILs were sourced from Sigma Aldrich. A couple of organic solvents were used in this investigation and they are methanol (purity ≥ 99.9%, Sigma Aldrich) and ethanol (purity ≥ 99.5%, Sigma Aldrich). Other chemicals employed in the experimental investigations include sulphuric acid (72 *w*/*w*%, RCI Labscan) and acetone (purity ≥ 99.9%, Sigma Aldrich).

Table 1 Proximate and ultimate analyses of untreated *RRG*

Proximate analysis (%)[a]				Ultimate analysis (%)[a]				
Moisture	Volatiles	Ash	Fixed carbon	C	H	N	S	O[b]
6.57 ± 0.21	80.71 ± 3.39	0.02 ± 0.003	12.7 ± 1.04	47 ± 1.65	5.47 ± 0.23	0.09 ± 0.006	0.06 ± 0.004	43.63 ± 3.14

[a] Values are on dry weight basis

[b] Values are on dry ash free basis

Biomass Pre-Treatment

IonoSolv Pre-Treatment

The IonoSolv pre-treatment was carried out in a 20ml vial. Initially, 0.5g oven dried *RRG* sample and 5 g IL were taken into the vial (*RRG* and IL in a 1:10 *w/w* ratio). In addition, 1 g distilled water was mixed with 5.5 g biomass-IL mixture when solid IL; [Bmim][Cl] was used. The weight of oven dried *RRG* sample was used as basis on the estimation of regenerated cellulose-rich material (*RCRM*).

The vial was immersed into a silicon oil bath as shown in the Supplementary Material (Fig. S1). The oil bath was placed on a magnetic stirrer (MR Hei-Standard, Heidolph Instruments) operating at 70 °C while providing a magnetic element stirring effect of 500 rpm in the oil. The pre-treatment was run for 3 h.

The pre-treated solution was then diluted with 50% (*v/v*) aqueous acetone. The ratio of pre-treated solution and aqueous acetone was 1:10 (*v/v*). The diluted solution was stirred at room temperature with a magnetic element at a speed of 500 rpm for 1 h. This stirring effect as well as chemical effect of acetone led to precipitate cellulose from the solution. The solution was centrifuged at 3000 rpm for 30 minutes and filtered through Whatman filter paper (pore size 6 μm) to collect the *RCRM*. While in filter paper, the solid *RCRM* was washed with distilled water to remove the residual IL. A conductivity meter (FiveEasy F30, Mettler Toledo) was employed in this investigation and the removal of ILs was confirmed by conductivity test of filtered water. When the conductivity of filtered water and the conductivity value of distilled water were very close, the washing of *RCRM* was terminated. The *RCRM* was dried overnight at 90 °C in a drying oven. It was then weighed employing a laboratory scale (Ohaus Pioneer PA114C, USA; readability 0.0001 g). The *RCRM* yield was calculated using Eq. (1).

$$\text{RCRM yield}\ (\%) = \frac{M_{\text{RCRM}}}{M_{\text{URB}}} \times 100 \tag{1}$$

where M_{RCRM} and M_{URB} indicate the mass of *RCRM* and the mass of untreated *RRG*, respectively.

The filtrate is a lignin-rich solution and lignin was separated from this solution by evaporating acetone. Once the evaporation of acetone is completed, the solution was centrifuged at 3000 rpm for 30 minutes and filtered through Whatman filter paper (pore size ≤2 μm). The separated lignin contains IL which needs to be removed. Similar to previous procedure, while in filter paper, lignin was washed with distilled water and the removal of IL was ensured by conductivity test. The lignin was dried overnight at 90 °C in a drying oven and its weight was measured gravimetrically. The degree of delignification was estimated by the following equation:

$$\text{Degree of delignification}\ (\%) = \frac{M_{\text{RL}}}{M_{\text{LURB}}} \times 100 \tag{2}$$

where M_{RL} and M_{LURB} indicate the mass of recovered lignin and the mass of lignin in untreated *RRG* respectively.

In this study, the TAPPI (Technical Association of the Pulp and Paper Industry) test method was applied on the determination of lignin content in the untreated *RRG*. This test procedure was established in a prior work [38]. The lignin content in the untreated *RRG* was found to be 29% and this value was used as M_{LURB} for the degree of delignification calculations.

The second filtrate (obtained after lignin separation) was constituted of hemicellulose, water and IL. This filtrate was initially heated to evaporate water from the solution. Ethanol (95%, *v/v*) was then added to this saturated solution in a ratio of 3:1 (*v/v*). Finally, the solution was centrifuged at 3000 rpm for 30 minutes and the solid hemicellulose was separated from the solution by filtration (Whatman filter paper, pore size ≤2 μm). The filtrate, obtained from this filtrated, was evaporated to recover IL. The recovered IL was kept overnight in a vacuum drying oven at 80 °C. The oven dried IL was ready to use for the next pre-treatment process. Once the IonoSolv pre-treatment of *RRG* was completed with one IL, the process was repeated with the other two ILs.

OrganoSolv Pre-Treatment

A solvent–water solution was initially prepared in a 50:50 volume ratio. In a 20ml vial, 0.5g oven dried *RRG* sample was mixed with the solvent–water solution in a ratio of 1:10 (*w/w*). The mixture-containing vial was heated for 3 h using an oil bath

and a magnetic stirrer as described in the IonoSolv pre-treatment process. After the completion of pre-treatment, the mixture was filtered through Whatman filter paper (pore size 6 μm) and the solid material was washed with distilled water ten times to ensure that the solvent was removed completely.

The filtrate obtained from this filtration contained lignin. In order to separate lignin from the filtrate solution, it was diluted with distilled water in a 3:1 (*w*/*w*) ratio and kept overnight to precipitate lignin. The temperature of distilled water was kept at 4 °C as suggested by a previous work [39]. The solution was centrifuged at 3000 rpm for 30 minutes and the solid lignin was separated from the solution by filtration using a Whatman filter paper (pore size ≤2 μm). The separated lignin was then washed with distilled water. The filtrate was concentrated by water evaporation. Hemicellulose was precipitated by adding 95% ethanol in a ratio of 3:1 (*v*/*v*) to this concentrated solution. The solution was centrifuged at 3000 rpm for 30 minutes and the solid hemicellulose was then separated by filtration (Whatman filter paper, pore size ≤2 μm). Both *RCRM* and lignin were dried overnight at 90 °C in a drying oven and their weights were measured. The organic solvent was not recovered. Once the *RRG* pre-treatment was completed by one organic solvent, the procedure was repeated with the other organic solvent.

Each experiment was repeated for three times. Thus, the data presented in the article represent the average values of the three experiments performed at identical conditions. Error bars are included where possible. These bars illustrate the maximum and minimum values from the average values.

Characterisation Methods

XRD Analysis

The crystalline and amorphous structures of untreated *RRG* and *RCRM* samples were analysed by a Bruker Axs D4 Endeavour Wide Angle X-Ray Diffraction instrument. The X-ray diffraction patterns of various samples were obtained at $2\theta = 6 - 40^{\circ}$ with a step size of 0.02°, a counting time of 0.3 s/step and divergent split of 1°. The instrument was operated at 40 kV voltage and 35 mA current. The *CrI* was estimated by using the XRD data and applying the following equation [6, 7, 40]:

$$\mathrm{CrI}\ (\%) = \frac{I_{002} - I_{\mathrm{am}}}{I_{002}} \times 100 \qquad (3)$$

where I_{002} refers to the maximum intensity of crystalline portion and I_{am} indicates the minimum intensity of amorphous region. I_{am} was estimated while capturing a XRD spectrum in the instrument. It is the intensity of the valley between I_{101} and I_{002} peaks with respect to baseline.

Thermogravimetric Analysis

Thermogravimetric analysis (TGA) of untreated *RRG* and *RCRM* samples was conducted by a STA 6000 Simultaneous Thermal Analyser (PerkinElmer, USA). The instrument was integrated with PerkinElmer Software Pyris®. This software was used in operating the instrument and collecting data. The sample was heated in a temperature range of 50–700 °C with a heating rate of 20 °C/min. Nitrogen was used as the TGA purge gas with a flow rate of 20 ml/min.

Scanning Electron Microscope Imaging and Analysis

The surface morphologies of untreated *RRG* and *RCRM* samples were examined by a scanning electron microscope (Philips XL30, USA). Prior to capture any SEM image, the specimen was placed on an aluminium stub with carbon tape and coated with gold using sputtered coating instrument. With the aim of comparing the surface morphology of untreated *RRG* and *RCRM* samples, the SEM images were obtained at the same spot size (5.0) and magnification (2000×). The SEM images were analysed using ImageJ software (version 1.46r), a public domain software developed by Wayne Rasband, National Institutes of Health, USA. In the software platform, the scale was initially set with a line of known length. Once the scale was set, it was used to determine pore diameter and pore area.

Fourier-Transform Infrared Spectroscopic Analysis

FTIR spectroscopic analyses of untreated *RRG* and *RCRM* samples as well as pure and recovered ILs were performed in a PerkinElmer FTIR Spectrometer (Spectrum 100, USA). FTIR spectra were captured in the scanning range of 4000–600 cm^{-1}.

For each experimental condition, the characterisation of materials was replicated. Thus, for each experimental condition, the characterisation of materials was performed for six times. This approach ensured that various figures and images presented in this article from material characterisation are reproducible.

Results and Discussion

RRG Dissolution and Degree of Delignification

The *RRG* dissolution capabilities of various ILs and organic solvents are illustrated in the Supplementary Material (Fig. S2). The darker colour IL pre-treated solutions suggest that ILs are more capable in *RRG* dissolution than organic solvents. It is expected that lignin, hemicellulose and cellulose of *RRG* can be dissolved in ILs while only lignin and

hemicellulose are dissolved in organic solvents. Hence, ILs show higher *RRG* dissolution capabilities compared to organic solvents. Similar findings are reported for other lignocellulosic biomass OrganoSolv pre-treatments in a previous work [13].

The IonoSolv pre-treatment processes transformed *RRG* into more fluffy structured materials when compared to OrganoSolv pre-treatments and this was confirmed by the apparent density measurements of *RCRM* samples as highlighted in Fig. 2. It can be seen that apparent densities of IonoSolv *RCRM* samples were reduced significantly when compared to untreated *RRG* or OrganoSolv *RCRM* samples. The gradual development of fluffy structured materials in IL pre-treatment of *RRG* assisted on the enhanced cellulose dissolution and lignin fragmentation [41].

We hypothesised that the dissolution of *RRG* in ILs might be attributed to the splitting of inter-unit linkages of lignin and dissolution of its constituents (i.e. cellulose, lignin and hemicellulose). It is previously established that both anions and cations play significant roles in the dissolution of biomass constituents [41]. During the pre-treatment process, ILs dissociate into cations such as $[Bmim]^+$ and $[Emim]^+$ and anions such as $[Cl]^-$ and $[OAc]^-$. Cations from ILs interact with polymeric molecules of lignin. In this process, electron-rich aromatic π-systems of IL cations involve in the interactions with π-systems of aromatic groups of lignin [42, 43]. In addition, IL anions can form H-bonds with hydrogen atoms of OH^- groups of lignin. The π–π interactions of IL cation–lignin and the formation of H-bonds by IL anions thus dissolve lignin polymers during IL pre-treatment processes. In the case of cellulose, it contains OH^- groups and IL anions interact with hydrogen atoms of OH^- groups of cellulose forming H-bonds. Hydrogen atoms of IL cations can also form H-bonds with the electronegative oxygen atoms of OH^- groups of cellulose [44]. The mechanism of dissolving hemicellulose is believed to be similar to that of cellulose dissolution [44].

As described in the methodology section, the dissolved cellulose in the IL pre-treatments was recovered by using antisolvent (aqueous acetone). In the case of OrganoSolv pre-treatment, the cellulose remained undissolved as described elsewhere [13] and therefore, no further treatment was required to recover the cellulose component.

The delignification performance of ILs and organic solvents is summarised in Fig. 3. The degree of delignification employing ILs was in the range of 21.4 to 26.2%. This pre-treatment result is in agreement with the previous works reported in the literature and described as follows. Doherty et al. studied the pre-treatment of maple wood flour at 90 °C employing [Emim][OAc] [45]. In their study, the degrees of

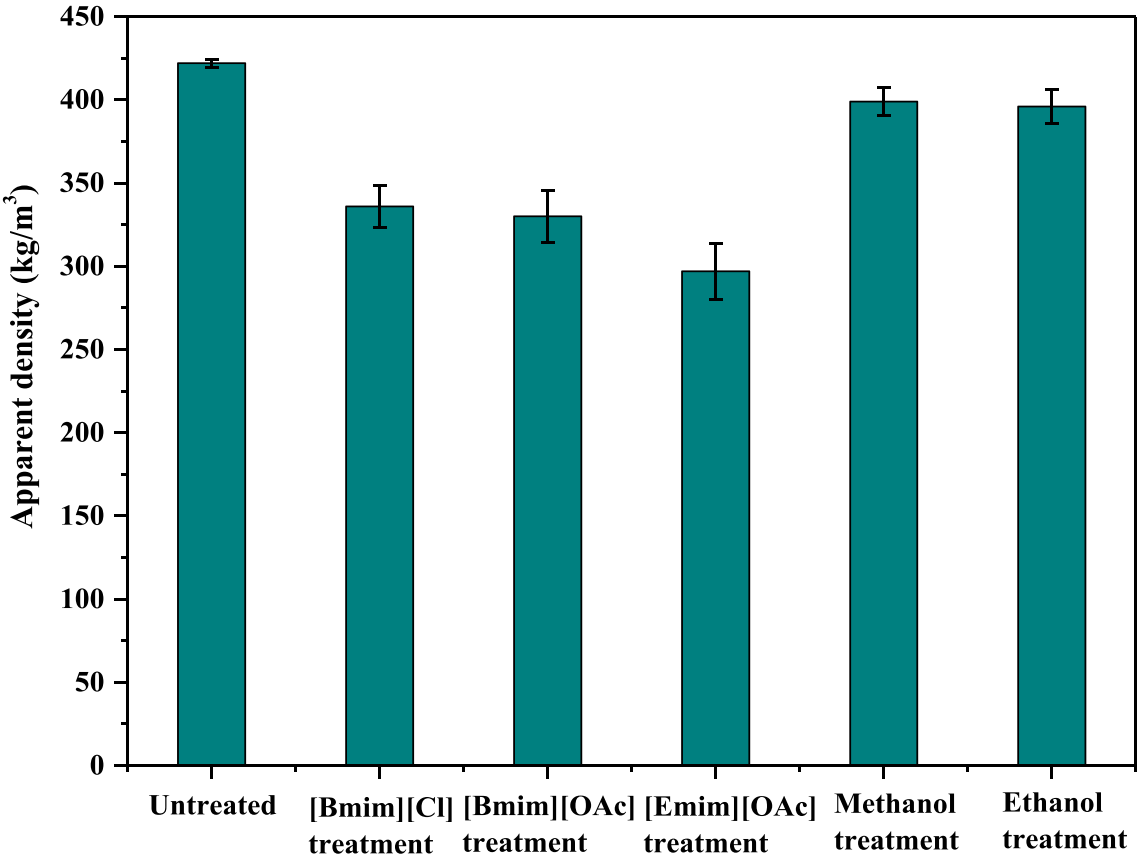

Fig. 2 Effect of pre-treatment method on *RCRM* apparent density

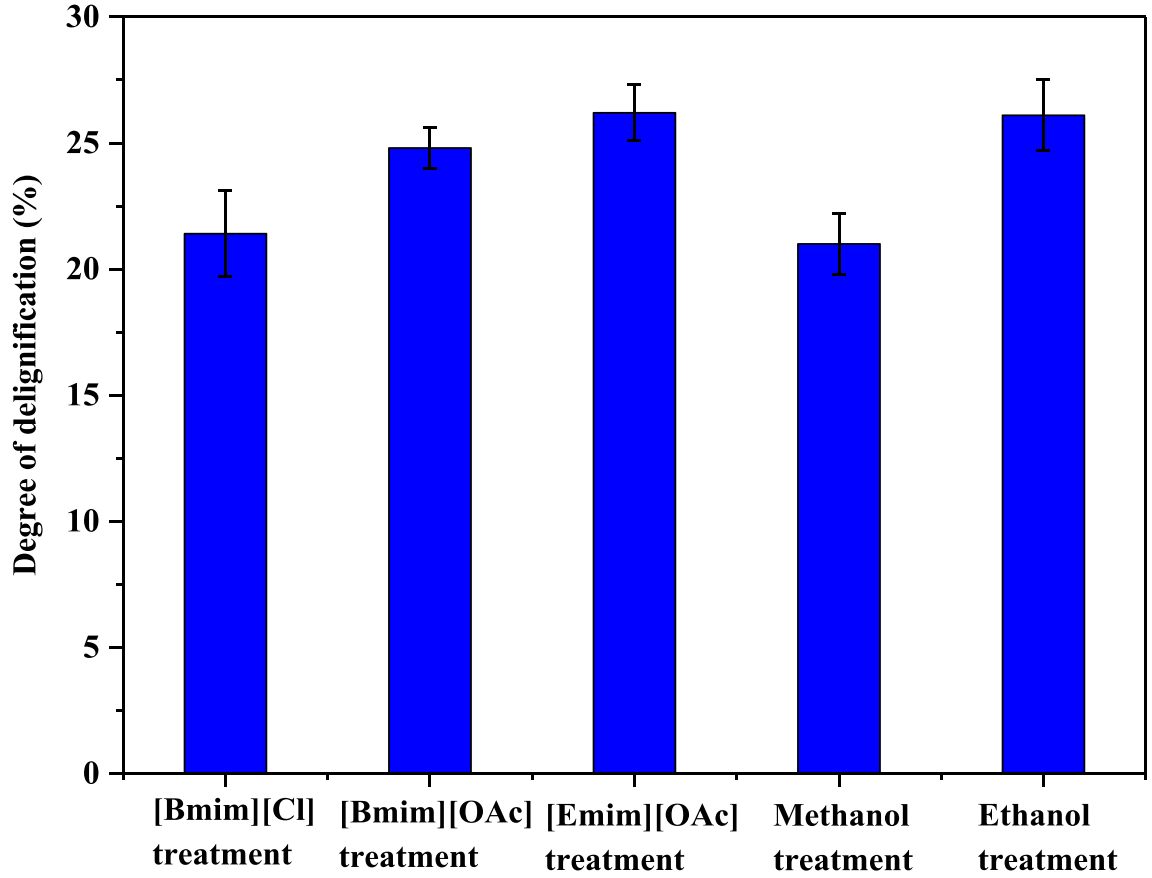

Fig. 3 Delignification performance of ILs and organic solvents on *RRG*

delignification were approximately 25, 35 and 49% for operating times of 6, 12 and 24 h respectively. When the wood flour was pre-treated with [Bmim][OAc] at same temperature, the degrees of delignification were approximately 26, 32 and 37% for 6, 12 and 24 h operating times, respectively. As evident in these results, the duration of pre-treatment is an important factor in the delignification process. Li et al. found that [Bmim][OAc] and [Bmim][Cl] can remove lignin from a hybrid biomass (*Eucalyptus urophylla x Eucalyptus grandis*) by 16.97 and 7.50%, respectively [32]. Their experiments were carried out at 120 °C for 30 min. The pre-treatment of southern yellow pine employing [Emim][OAc] at 110 °C for 16 h showed 26.1% reduction of lignin in the pre-treated material [38], and this degree of delignification was nearly similar to the present study (26.2%). Heggset et al. pre-treated Norway spruce chips with [Emim][OAc] at 100 °C for 6 h and the study showed nearly 31.7% lignin reduction in the pre-treated material [46]. Mohtar et al. observed approximately 54% lignin reduction in pre-treated material obtained from the [Bmim][Cl] pre-treatment of oil palm biomass for 8 h at 110 °C in N_2 environment [33]. The process temperature is also an important factor that impacts the degree of delignification. When relatively higher process temperature (175 °C) was applied on the pre-treatment of southern yellow pine with [Emim][OAc], a higher value of lignin (49.4%) was separated within a short pre-treatment duration of 30 min (comparative result in that study 26.1% lignin separation at 110 °C for 16 h) [47]. The lignin content in the *RCRM*, obtained from the pre-treatment of maple wood flour with [Emim][OAc], was found to be reduced by more than 85% when the raw biomass material was pre-treated for 70 h at 90 °C in N_2 environment [16]. It can be seen from the above discussions that the degrees of delignification values obtained in the present study are comparable with several previous studies. However, variations are also observed on the degrees of delignification values. Those variations of delignification efficiencies may be attributed to the differences in pre-treatment conditions and biomass structures.

In the case of organic solvents, ethanol removed more lignin from *RRG* than methanol. The degree of delignification values for methanol and ethanol pre-treatments was 21 and 26.1%, respectively and these values are in agreement with a recent study on the pre-treatment of eucalyptus chips with ethanol (concentration 60%) [14]. The eucalyptus chips pre-treatment study was conducted at 160 °C for 90 min and an extraction of 21.7% lignin was reported.

When comparing IonoSolv and OrganoSolv pre-treatments, it can be concluded that the delignification efficiency

of ethanol solvent was very similar to that of [Emim][OAc] pre-treatment (26.2%). According to the degree of delignification values obtained from the current investigation, the employed ILs can be ordered as follows: [Emim][OAc] > [Bmim][OAc] > [Bmim][Cl]. This finding suggests that ILs having acetate ($[OAc]^-$) anions are superior in lignin dissolution than that of chloride ($[Cl]^-$) anions. This was mainly because the hydrogen bond basicity of $[OAc]^-$ anions is higher than that of $[Cl]^-$ anions [44, 45, 48]. Hydrogen bond basicity of a particular molecule refers to the ability of that molecule to accept protons [49]. The higher hydrogen bond basicity of $[OAc]^-$ anions enhances the formation of H-bonds between IL anions and hydroxyl ($[OH]^-$) groups of lignin. Between two IL cations, employed in this investigation, $[Bmim]^+$ is heavier than $[Emim]^+$. The shorter $[Emim]^+$ ion is more mobile than $[Bmim]^+$ ion in the reaction environment [17, 50]. Thus, $[Emim]^+$ ion-containing ILs can show higher delignification capability than that of $[Bmim]^+$ ion-containing ILs.

Figure 4 shows the average mass compositions of hemicellulose, lignin and *RCRM* components. It can be seen from the figure that the percentage of lignin removal was ranged from 6.2 to 7.6% while the *RCRM* yields were between 90.4 and 92.4%. Additionally, the pre-treatment processes removed hemicellulose with values between 1.0 to 1.8% of untreated *RRG*. The corresponding mass values of the separated hemicellulose were too low for further analysis. A small mass loss was observed in each pre-treatment experiment and the values of mass loss varied from 0.1 to 0.3% of untreated *RRG*. This level of mass loss is supported by previous works [51, 52]. Brandt-Talbot et al. [51] reported noticeable mass loss (> 10%) during the pre-treatment of *Miscanthus x giganteus* biomass using triethylammonium hydrogen sulphate. Similar observations are reported by a different study on the discrepancy of mass balance [52].

Characterisation of Untreated *RRG* and *RCRM* Samples

XRD and *CrI* Analysis

Figure 5 illustrates XRD spectra of untreated *RRG* and *RCRM* samples. The *CrI* values presented in this figure are average *CrI* values from three experiments. In the untreated sample spectra, three diffraction peaks were observed with 2θ values of 15.6°, 22.5° and 34.5° corresponding to lattice plane I_{101}, I_{002} and I_{040}, respectively. These three peaks represent the native crystalline cellulose which is also known as cellulose I. These findings are supported by a previous work which reported the presence of cellulose I at $2\theta = 15.8^{\circ}$, $2\theta = 22.3^{\circ}$

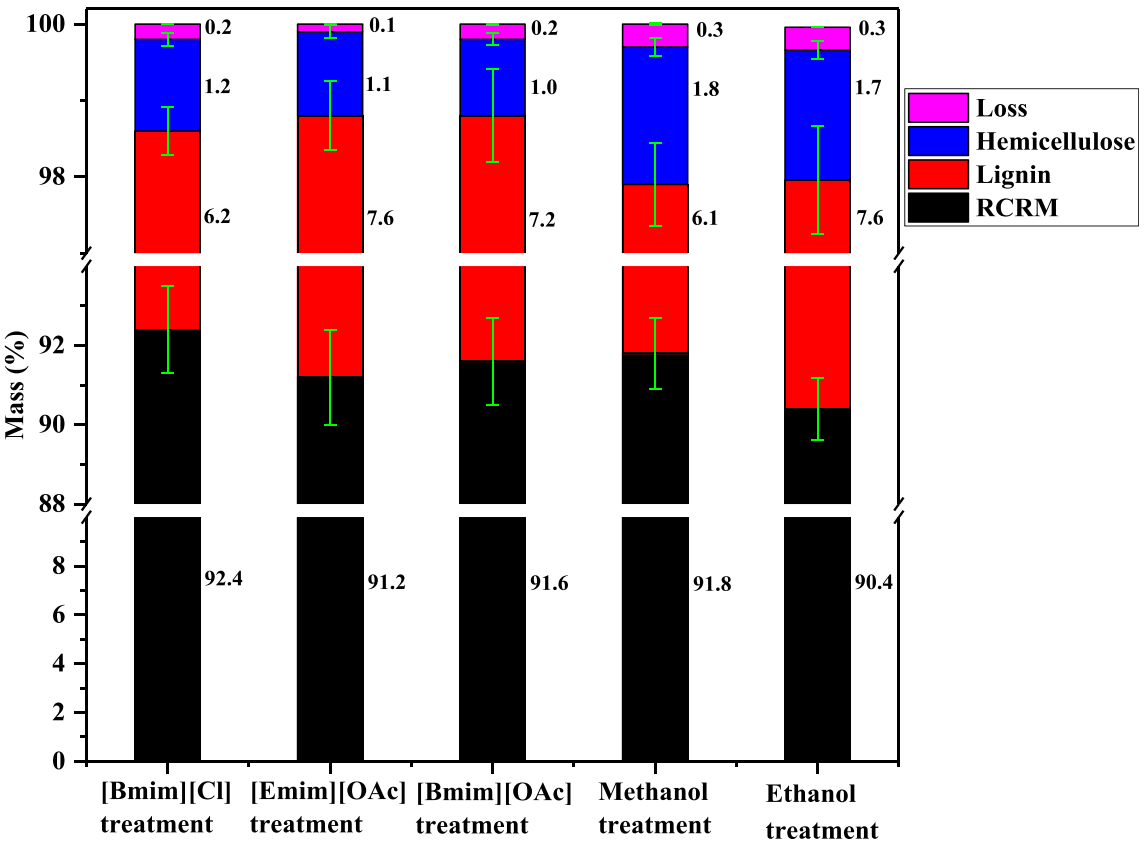

Fig. 4 Mass balance of various fractions obtained from IonoSolv and OrganoSolv pre-treatments of *RRG*

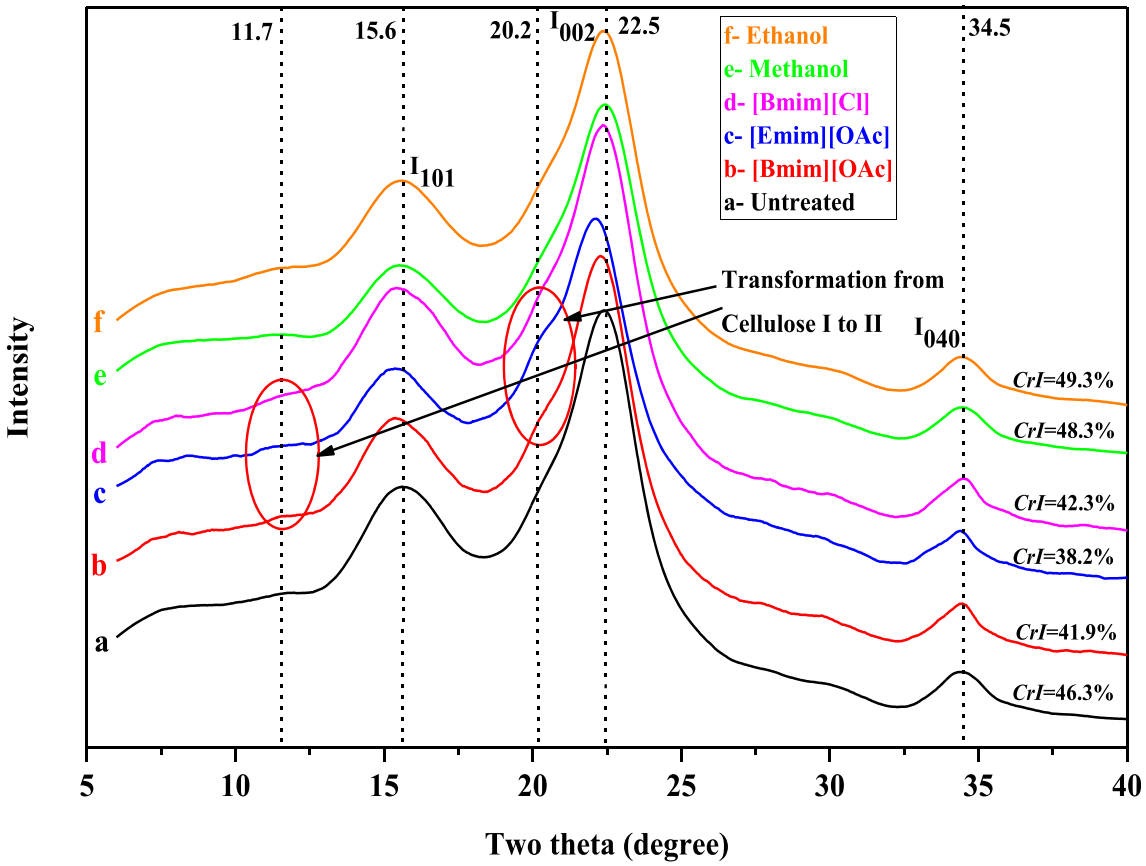

Fig. 5 XRD spectra of untreated *RRG* and *RCRM* samples

and $2\theta = 34.3^{\circ}$ [32]. According to the XRD measurements obtained in the present investigation, the *CrI* value of untreated *RRG* was 46.3%. When the *RRG* was pre-treated with ILs, the *CrI* values of IonoSolv *RCRM* samples dropped to 38.2, 41.9 and 42.3% for [Emim][OAc], [Bmim][OAc] and [Bmim][Cl], respectively. As a result of IL pre-treatments, the peaks at the lattice planes I_{002} and I_{101} shifted towards lower angles and the intensities of those peaks were reduced. The highest change in peak shift (i.e. 22.5 to 22.1° and 15.6 to 15.3°) was observed in the case of [Emim][OAc] treatment. The peak shift and the reduction of the peak intensity were attributed to lead the disruption of cellulose structure as well as the transformation of cellulose I to cellulose II [53].

Two new weak XRD peaks were observed at 11.7° and 20.2° angles in the case of IonoSolv pre-treatments. These peaks refer to cellulose II illustrating the transformation of cellulose I to cellulose II [53, 54]. The transformation of cellulose I to cellulose II was responsible for the decrease in *CrI* for IonoSolv *RCRM* samples. When the *RRG* was pre-treated with organic solvents, the values of *CrI* were found to be increased in the *RCRM* samples. The increase in *CrI* in OrganoSolv *RCRM* was due to the separations of amorphous lignin and hemicellulose from *RRG* as supported by a previous work [14]. The separations of lignin and hemicellulose from biomass also occur in the case of IonoSolv pre-treatments; however, the impact of the transformation of cellulose I to cellulose II on *CrI* values is higher than that of the separations of lignin and hemicellulose from biomass in the IL pre-treatments. It can be seen from Fig. 5 that there is no new development of XRD peaks for OrganoSolv *RCRM* samples and this indicates that cellulose I may be unchanged in the OrganoSolv *RCRM* samples.

FTIR Spectroscopic Analysis

Figure 6 shows FTIR spectra of untreated *RRG* and *RCRM* samples. In the case of untreated sample, the peaks appeared at 3342, 2900, 1734, 1505, 1422, 1228 and 1028 cm^{-1} indicate OH stretching in cellulose, C–H stretch in cellulose, C=O unconjugated stretching in hemicellulose, C=C aromatic symmetrical stretching in lignin, C=C stretching in lignin and hemicellulose, C=O stretching in lignin and hemicellulose and C–O stretching in cellulose, respectively [53–55]. The peak intensity at 1505 and 1422 cm^{-1} decreased for the all *RCRM* samples indicating the partial removal of lignin and hemicellulose during pre-treatment. In the case of IonoSolv *RCRM* samples, two new peaks are observed at 3265 and 1267 cm^{-1} and their appearance is due to the results of the

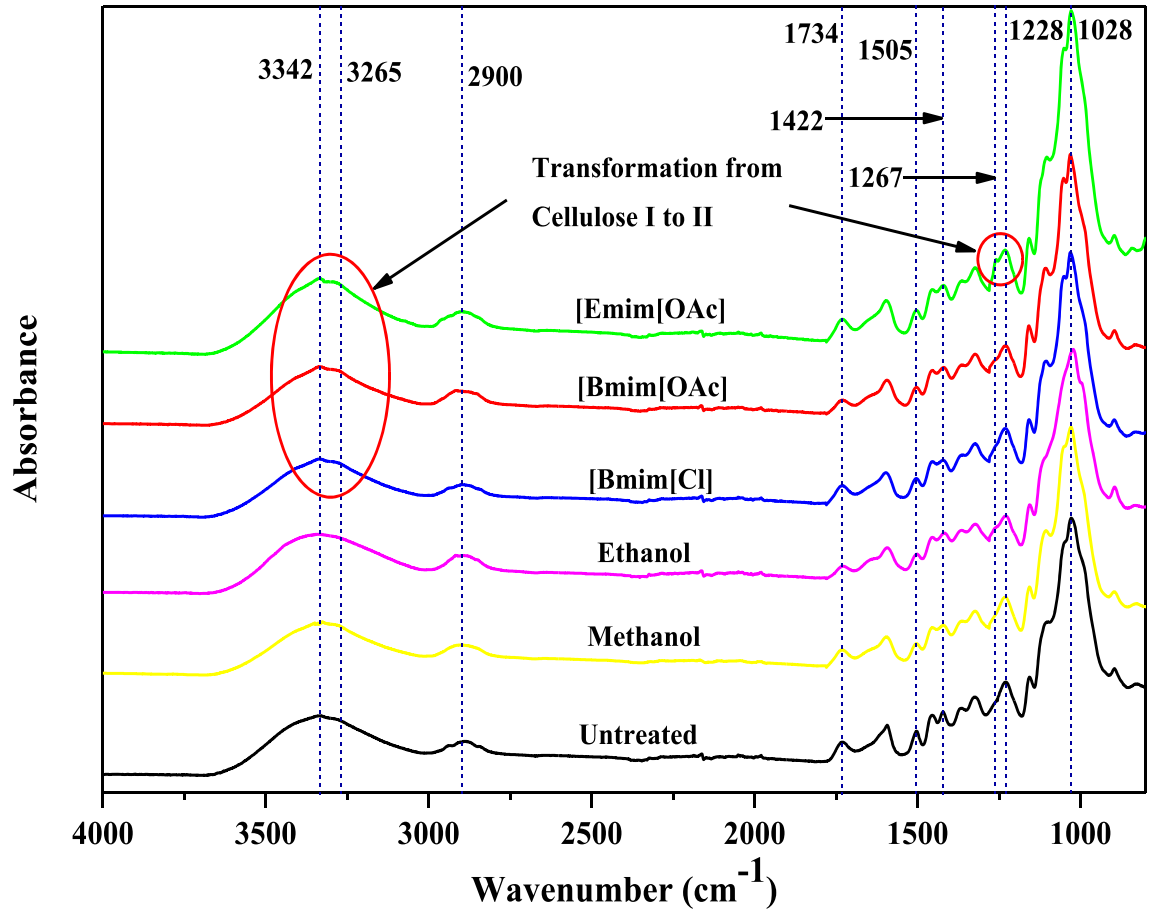

Fig. 6 FTIR spectra of untreated *RRG* and *RCRM* samples

disruptions of H-bonds in cellulose and the transformation of cellulose I to cellulose II [53, 56]. This result is in accordance with the XRD measurements as discussed earlier. This effect was highly pronounced in the [Emim][OAc] pre-treatment. Similar to the XRD measurements, no cellulose II structure was observed in the OrganoSolv *RCRM* samples.

Relative Change in *CrI*

Figure 7 shows the relative change in *CrI* (with respect to *CrI* of untreated *RRG*) for the IonoSolv and OrganoSolv *RCRM* samples. In contrast to OrganoSolv *RCRM* samples, *CrI* was found to be decreased in the case of IonoSolv pre-treatment. [Emim][OAc] exhibited the maximum reduction in *CrI* with a value of 17.4%. Similar findings are reported in the literature for the [Emim][OAc] treatment of wood flour with a relative reduction in *CrI* value of 17.5% [16]. As described earlier, OrganoSolv pre-treatment increased the *CrI* value of *RRG*. For example, the relative change in *CrI* of *RCRM* for ethanol pre-treatment was found to be 6.6%. A similar finding was reported for the pre-treatment of eucalyptus with ethanol (concentration 60%), where *CrI* of eucalyptus increased 5.2% with respect to *CrI* of untreated eucalyptus [14]. In the present study, ethanol pre-treatment showed higher increase in *CrI* than that of methanol.

Overall, it can be summarised that an increase in the degree of delignification is observed for IonoSolv pre-treatments and this is linked to the decrease in the *CrI*. This suggests that a fraction of crystalline cellulose I converts to amorphous cellulose II during IL pre-treatment process. It has been reported previously that the effectiveness of enzymatic hydrolysis of biomass is strongly correlated with *CrI* of biomass material [16, 57]. For instance, Lee et al. reported that the enzymatic hydrolysis of maple wood was increased when the maple wood was pre-treated with [Emim][OAc] leading to the reduction of *CrI* values [16]. Figure 8 shows the relative increase in enzymatic hydrolysis (with respect to enzymatic hydrolysis of untreated maple wood) against the relative reduction of *CrI* (with respect to *CrI* of untreated maple wood). Taking into account the hydrolysis trend of Lee et al. [16], *CrI* value of the present study can be linked to the hydrolysis efficiency (Fig. 8). Accordingly, it may be predicted that the low temperature (70 °C) [Emim][OAc] pre-treatment of *RRG* employed in this study can increase the hydrolysis efficiency of *RCRM*. As can be seen from the Fig. 8, the relative increase in hydrolysis of *RCRM* is expected approximately 26.1% with respect

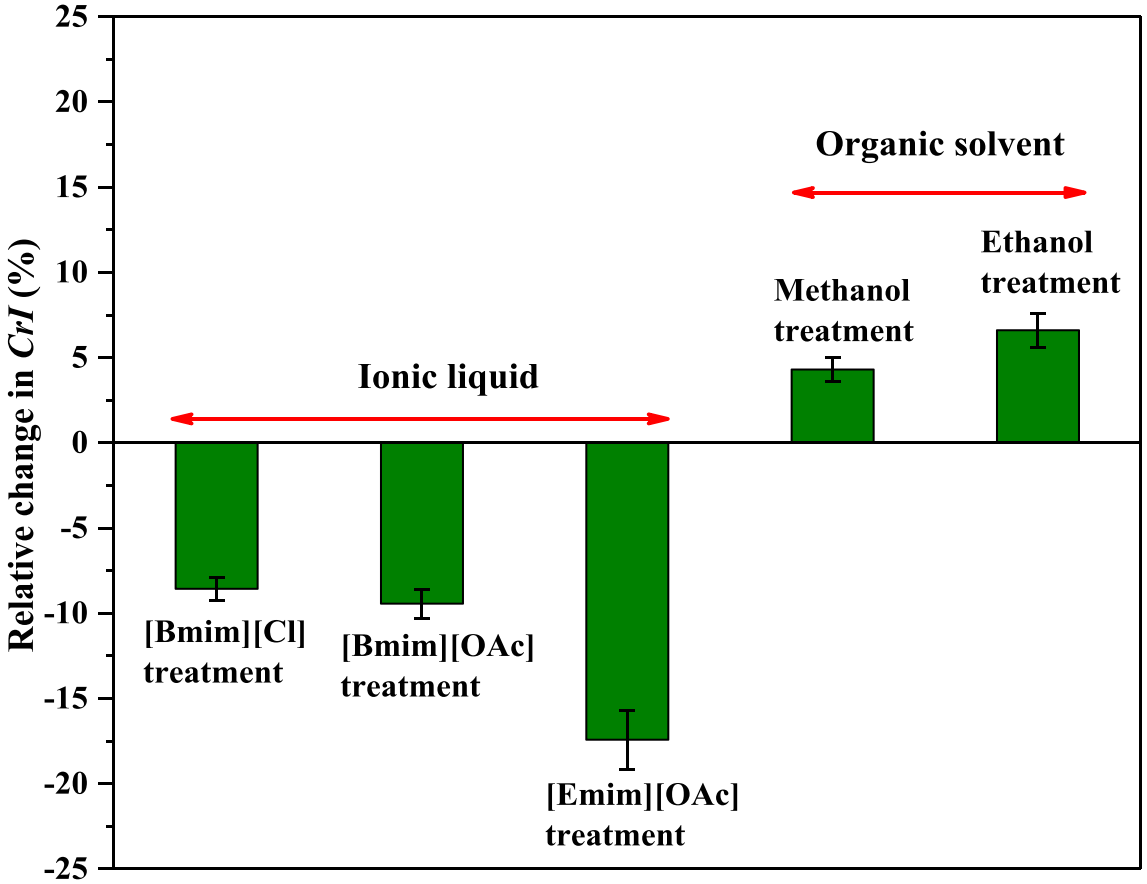

Fig. 7 Relative change of *CrI* for IonoSolv and OrganoSolv *RCRM* samples with respect to untreated *RRG CrI*

to that of untreated *RRG*. The lower value of *CrI* is also favourable for thermochemical conversion of biomass [58].

Thermogravimetric Analysis

Figure 9a, b show the thermogravimetric analysis (TGA) and derivative thermogravimetric (DTG) analyses respectively for untreated *RRG* and *RCRM* samples (TGA profiles with repeat data are presented in the Supplementary Material in Fig. S3). Notable changes are observed in the thermal profiles of untreated *RRG* and *RCRM* samples as shown in Fig. 9a. These changes were attributed to the physicochemical transformations occurred during the IonoSolv and OrganoSolv pre-treatments. To gain deeper understanding, DTG plots provided in Fig. 9b are analysed. In general, three peaks are observed for both untreated *RRG* and *RCRM* samples. The first peak is believed to be the dehydration phase (70–80 °C) and it indicates mainly moisture removal. The second and third peaks are assumed to be the thermal decomposition of hemicellulose (250–290 °C) and cellulose (350–380 °C), respectively [59]. The decomposition of lignin is expected to extend throughout the hemicellulose and cellulose region (200 to 700 °C) as reported previously [59]. Therefore, no separate peak is observed for lignin in Fig. 9b. Noticeable differences are observed between the IonoSolv and OrganoSolv *RCRM* samples in the decomposition temperatures of cellulose and hemicellulose. With respect to untreated *RRG* and OrganoSolv *RCRM* samples, the decomposition temperatures are found to be shifted slightly towards a lower temperature for IonoSolv *RCRM* samples. This observation is highly pronounced in the *RCRM* sample obtained from [Emim][OAc] pre-treatment which has shown the lowest *CrI* and the highest intensity. This further confirms the physicochemical alterations, decrease in *CrI* and conversion of cellulose I to cellulose II in IonoSolv *RCRM* samples

Surface Morphology Analysis

The morphological changes in *RRG* during IonoSolv and OrganoSolv pre-treatments are presented in Fig. 10 (SEM images with repeat data are presented in the Supplementary Material in Fig. S4). As described in the "Experimental" section, the SEM images were captured at the same spot size and magnification. This provides a visual comparison amongst untreated *RRG* and *RCRM* samples. The untreated *RRG* was observed to be compact, regularly ordered and intact structure

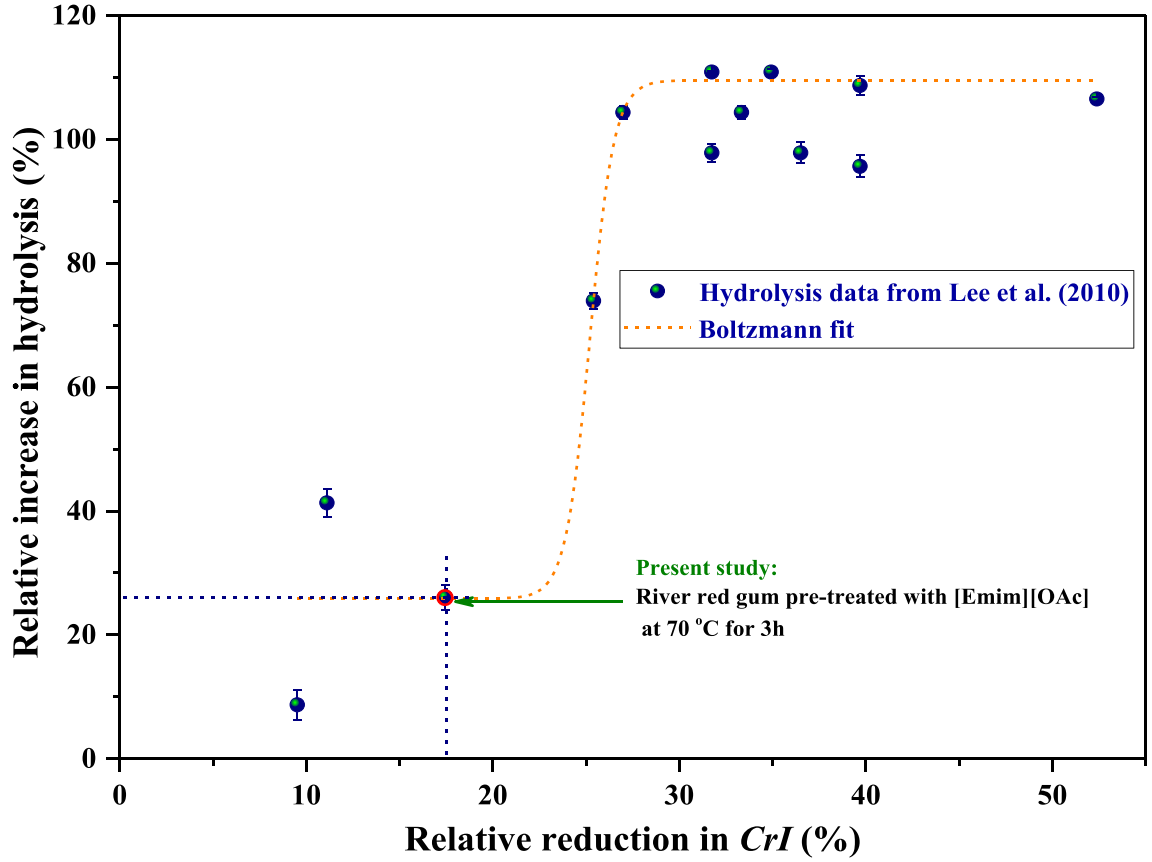

Fig. 8 Correlation between enzymatic hydrolysis and *CrI* of biomass [16]

with no pores on the surface (Fig. 10a). This was due to the presence of lignin polymers as these polymers act as glue coating and surround cellulose and hemicellulose forming rigid structure [2]. The IonoSolv and OrganoSolv pre-treatments removed lignin and hemicellulose from lignocellulosic structure and modified the surface morphologies of *RCRM* samples. Both organic solvents exhibited mainly thinning effects as shown in Fig. 10b and c. In contrast, IL pre-treatment, along with thinning, developed pores in the *RRG* structures as evident in Fig. 10d–f. The maximum pore area in *RCRM* samples yielded from [Emim][OAc], [Bmim][OAc] and [Bmim][Cl] pre-treatments was approximately 182.5, 172.2 and 53.4 μm^2, respectively (the estimated pore areas considered the top flat area of a pore). The deconstruction of the lignocellulosic structure and washing out of materials is responsible for the thinning of the structure in both IonoSolv and OrganoSolv pre-treatments while the pore development in IL pre-treatment is attributed to the transformation of cellulose I to cellulose II.

Figure 11 represents a comparative analysis on pore size (the maximum diameter of the top flat area of a pore) in the IonoSolv *RCRM* samples. The porous structures of *RCRM* samples favour their hydrolysis and biodigestibility for biofuel production [12]. In terms of pore development, the ILs can be organised as follows: [Emim][OAc] > [Bmim][OAc] > [Bmim][Cl]. As explained earlier, such trend is observed due to higher hydrogen bond basicity of $[OAc]^-$ anions compared to $[Cl]^-$ anions and higher mobility of shorter $[Emim]^+$ cations compared to $[Bmim]^+$ cations.

Recovery of Ionic Liquid

The cost of IL is considered to be the main impediment for the commercial applications of ILs in biomass pre-treatments [60]. Nevertheless, ILs, due to their low vapour pressures, can be regenerated which can significantly reduce the cost of biomass pre-treatment. In this study, ILs were recovered after the pre-treatments and the structural changes were analysed by FTIR spectrometer. The recovery percentage of [Emim][OAc], [Bmim][Cl] and [Bmim][OAc] were 88.2, 83.6 and 87.4%, respectively. These values are in agreement with previous studies that reported the recovery of [Emim][OAc] and [Emim][DEP] to be 89 and 90% respectively for the pre-treatments of corn stover and oil palm frond [61, 62]. However, the percentage recovery of ILs and performance of recovered ILs on biomass dissolution is largely dependent on the method employed for the recovery [63, 64]. For instance, Liang et al. recovered [Amim][Cl] (1-allyl-3-methylimidazolium chloride) using membrane-based electrodialysis method and used the recovered IL for 5 cycles in the

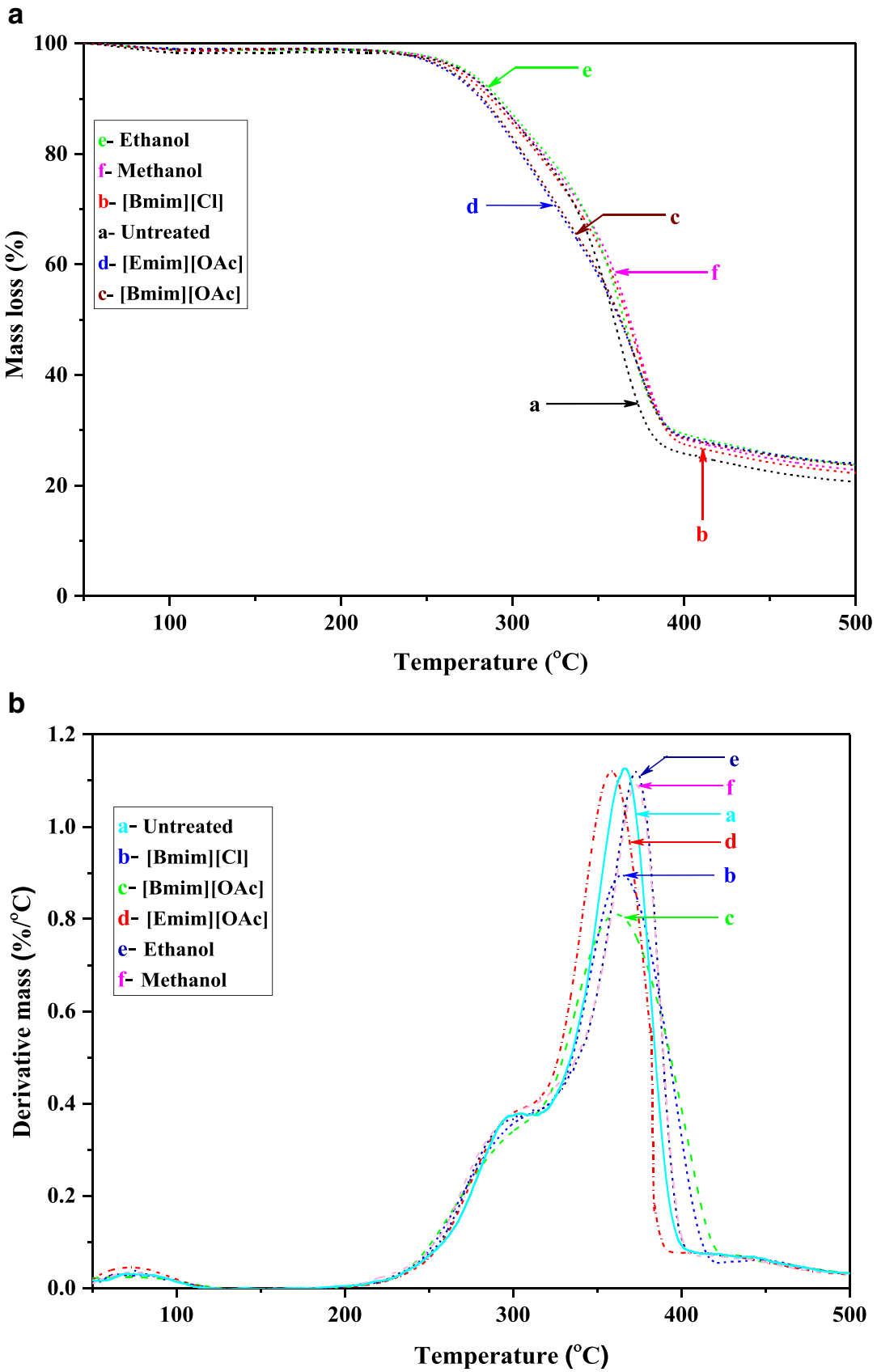

Fig. 9 Thermal decomposition behaviour of untreated *RRG* and *RCRM* samples **a** TGA profiles **b** DTG thermograms

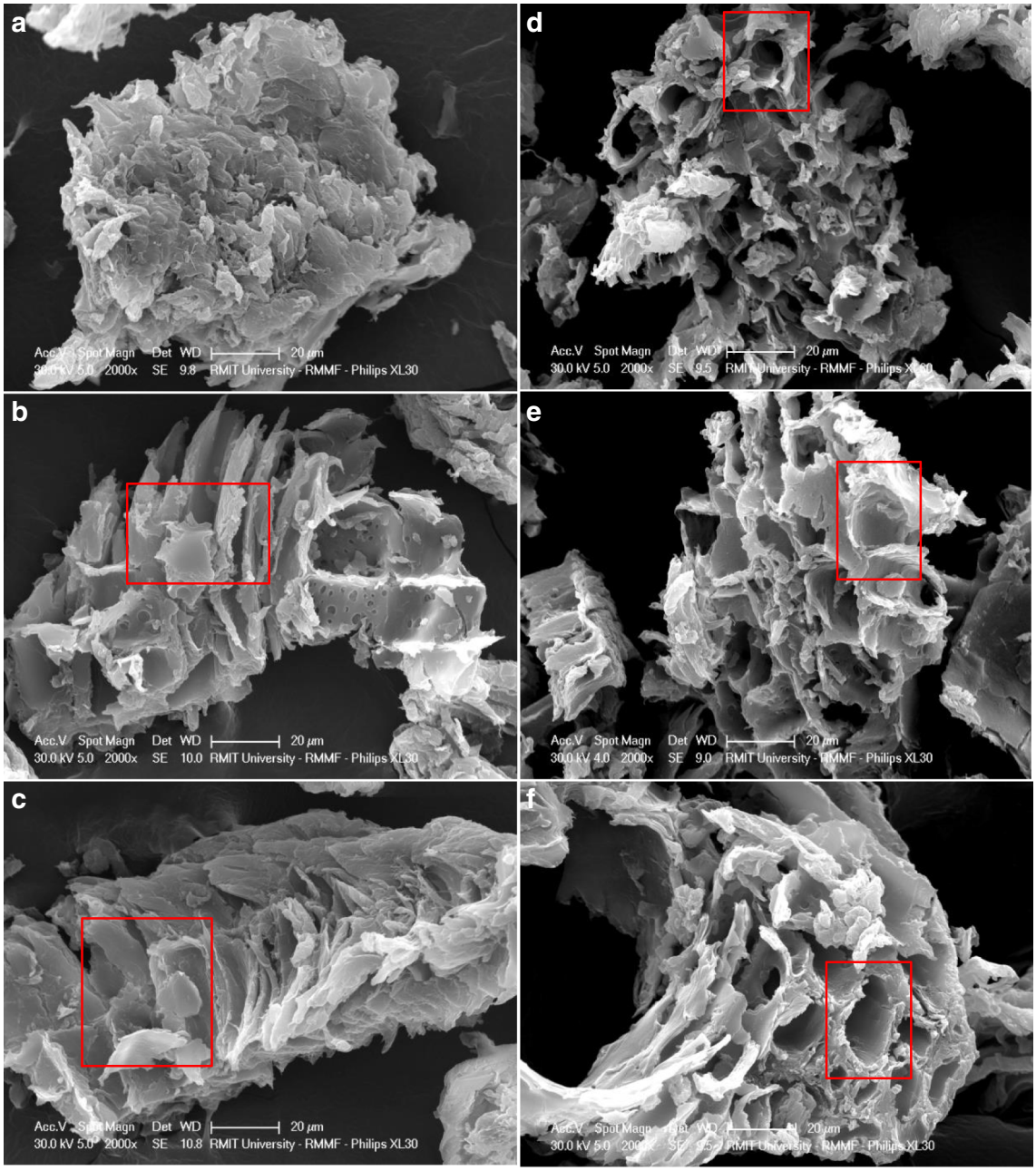

Fig. 10 SEM images of **a** untreated *RRG*, **b** *RCRM* from methanol pre-treatment, **c** *RCRM* from ethanol pre-treatment, **d** *RCRM* from [Bmim][Cl] pre-treatment, **e** *RCRM* from [Bmim][OAc] pre-treatment and **f** *RCRM* from [Emim][OAc] pre-treatment

pre-treatment of *Eucalyptus globulus* [65]. They observed that the recovered IL showed almost the same dissolution capability when compared that to fresh IL. Hou et al. observed a minor reduction in lignin separation capability of [Ch][Ly] (cholinium lysine) when the IL was recovered and reused over five times [66]. These highlight the recyclability of ILs and the commercial suitability of IonoSolv pre-treatment processes.

The FTIR spectra of pure and recovered ILs, obtained from the present study, are provided in the Supplementary Material (Fig. S5). It can be seen from Fig. S5 that pure ILs show three peaks in the spectral region of 3000–2800 cm^{-1} indicating the stretching of alkyl C–H bands [67–70]. These peaks can be traced at 2863, 2917 and 2977 cm^{-1} for pure [Emim][OAc]; 2868, 2934 and 2963 cm^{-1} for pure [Bmim][OAc] and 2870, 2932 and 2957 cm^{-1} for pure [Bmim][Cl], respectively. In the spectral region of 3200–3000 cm^{-1}, two imidazolium C-H stretching bands can be observed at 3055 and 3144 cm^{-1} for pure [Emim][OAc]. Similar imidazolium C–H stretching bands are identified at 3073 and 3142 cm^{-1} for pure [Bmim][OAc] and 3090 and 3149 cm^{-1} for pure [Bmim][Cl] [67–70]. The broad peak in the region of 3400 cm^{-1} can be assigned to O–H stretching bands [67]. The absorption peaks

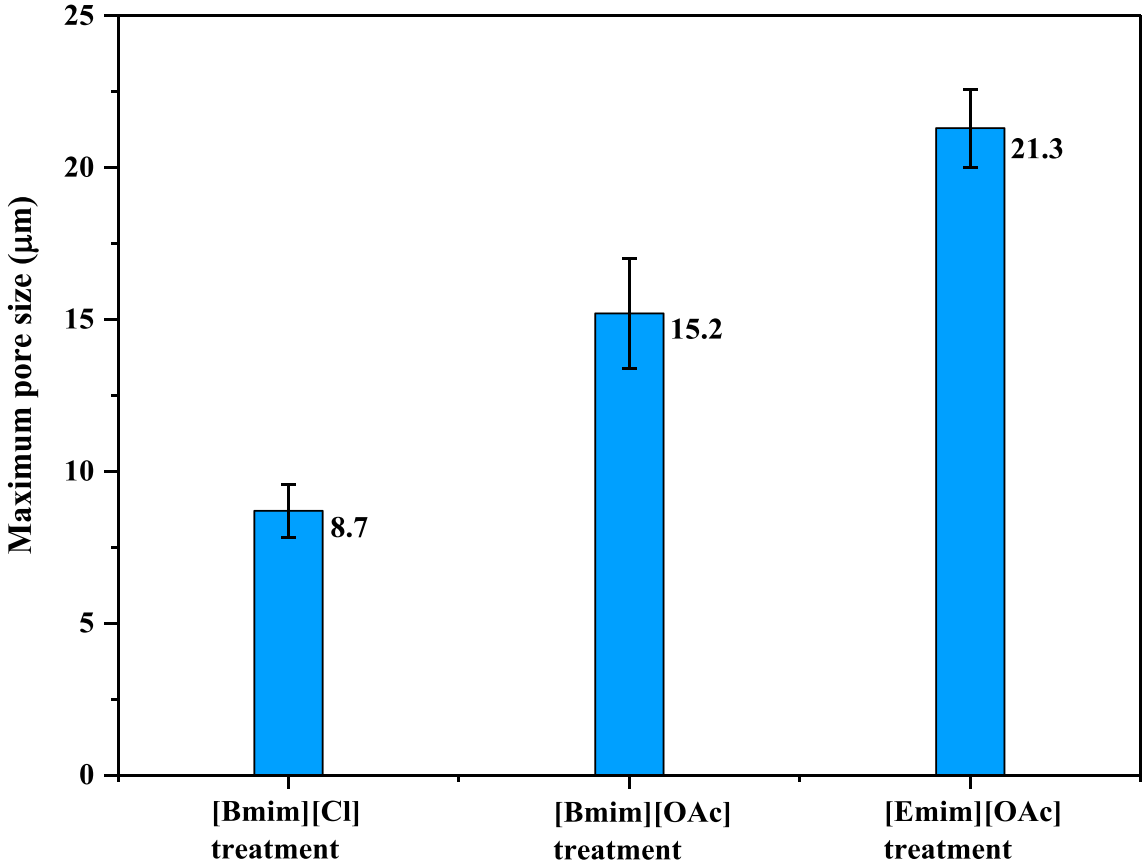

Fig. 11 The size variation of developed pores in IonoSolv *RCRM* samples

at 1175, 1377 and 1563 cm^{-1} for pure [Emim][OAc]; 1171, 1379 and 1563 cm^{-1} for pure [Bmim][OAc] and 1170, 1461 and 1566 cm^{-1} for pure [Bmim][Cl] are assigned to symmetric O–C–O, asymmetric O–C–O and C–O stretching, respectively [71]. In the recovered [Bmim][Cl], the imidazolium C–H stretching band is shifted from 3090 to 3045 cm^{-1} and it is due to changes in local geometry caused by H-bonding [68] as illustrated in Fig. S5c. In the case of recovered [Emim][OAc], two broad O–H stretching peaks are observed at 3396 and 1660 cm^{-1} wavenumbers indicating the presence of moisture in recovered IL. Similarly, O–H stretching peak is identified at 1640 cm^{-1} wavenumber for the recovered [Bmim][Cl]. Similar to the FTIR analysis of this study, the presence of O–H group was observed in the FTIR spectrum of the recovered [Bmim][Cl] employed in the pre-treatment of coal [72]. Briefly, the FTIR spectral analysis suggests that there are no noticeable differences in the FTIR spectra of the recovered and the pure ILs.

Conclusion

The low temperature pre-treatments (i.e. 70 °C for 3 h) of *RRG* were studied employing ILs and organic solvents with the aim of separating lignin from cellulose-rich material (i.e. delignification).

By applying IL and organic solvent pre-treatments, more than 20% lignin was removed from *RRG* in this investigation. According to the delignification capabilities, the ILs can be ordered as follows: [Emim][OAc] > [Bmim][OAc] > [Bmim][Cl]. The higher delignification performance of [Emim][OAc] is observed due to higher hydrogen bond basicity of $[OAc]^-$ anions compared to $[Cl]^-$ anions and higher mobility of shorter $[Emim]^+$ cations compared to $[Bmim]^+$ cations. For organic solvents, ethanol was found to be working better than methanol for the delignification of *RRG*.

The IL pre-treatments were able to reduce *CrI* in the IonoSolv *RCRM* samples while *CrI* was found to be increased in OrganoSolv *RCRM* samples. Such differences are attributed to the conversion of crystalline cellulose I to amorphous cellulose II during IL pre-treatments and this phenomenon has not been observed in the case of organic solvent pre-treatments.

IonoSolv pre-treatments are found to produce pores in the regenerated cellulose-rich material fractions. According to pore size (from large to small) in *RCRM* samples, the order of ILs is as follows: [Emim][OAc] > [Bmim][OAc] >

[Bmim][Cl]. In the case of OrganoSolv pre-treatments, no noticeable pore is observed in the *RCRM* samples.

[Emim][OAc], [Bmim][Cl] and [Bmim][OAc] were recovered with recovery values of 88.2, 83.6 and 87.4%, respectively. According to FTIR spectral analysis, a minor structural alteration was observed in the recovered [Bmim][Cl] when compared to the pure [Bmim][Cl]. No structural change was observed in the case of recovered [Emim][OAc] and [Bmim][OAc]. This establishes their recyclability and indicates that the ILs can be used cost effectively for low temperature *RRG* pre-treatments.

Acknowledgements This work was supported by the School of Engineering, RMIT University, Melbourne, Australia. The first and third authors are indebted to the School of Engineering, RMIT University for their postgraduate scholarships.

Compliance with Ethical Standards

Conflict of Interest The authors declare that they have no conflict of interest.

References

1. de Carvalho DM, Sevastyanova O, de Queiroz JH, Colodette JL (2016) Cold alkaline extraction as a pretreatment for bioethanol production from eucalyptus, sugarcane bagasse and sugarcane straw. Energy Convers Manag 124:315–324
2. Yin C (2012) Microwave-assisted pyrolysis of biomass for liquid biofuels production. Bioresour Technol 120:273–284
3. Crawford DF, O'Connor MH, Jovanovic T et al (2016) A spatial assessment of potential biomass for bioenergy in Australia in 2010, and possible expansion by 2030 and 2050. GCB Bioenergy 8:707–722
4. Davis L (2002) Multiple benefits from bio-fuels. In: Adelaide Firewood Conference. pp 156–158
5. Pereira BLC, Carneirode A de CO, Carvalho AMML et al (2013) Influence of chemical composition of Eucalyptus wood on gravimetric yield and charcoal properties. BioResources 8:4574–4592
6. Morais D, Carvalho D, Sevastyanova O et al (2015) Assessment of chemical transformations in eucalyptus, sugarcane bagasse and straw during hydrothermal, dilute acid, and alkaline pretreatments. Ind Crop Prod 73:118–126
7. Yu Q, Zhuang X, Yuan Z, Wang Q, Qi W, Wang W, Zhang Y, Xu J, Xu H (2010) Two-step liquid hot water pretreatment of Eucalyptus grandis to enhance sugar recovery and enzymatic digestibility of cellulose. Bioresour Technol 101:4895–4899
8. Elena M, Cristina M, Pezoa-conte R et al (2016) Second generation bioethanol from Eucalyptus globulus Labill and Nothofagus pumilio: ionic liquid pretreatment boosts the yields. Ind Crop Prod 80:148–155
9. Romaní A, Ruiz HA, Teixeira JA, Domingues L (2016) Valorization of Eucalyptus wood by glycerol-organosolv pretreatment within the biorefinery concept: an integrated and intensified approach. Renew Energy 95:1–9
10. Percival Zhang Y-H, Berson E, Sarkanen S, Dale BE (2009) Pretreatment and biomass recalcitrance: fundamentals and Progress. Appl Biochem Biotechnol 153:80–83
11. Agbor VB, Cicek N, Sparling R, Berlin A, Levin DB (2011) Biomass pretreatment: fundamentals toward application. Biotechnol Adv 29:675–685
12. Taherzadeh MJ, Karimi K (2008) Pretreatment of lignocellulosic wastes to improve ethanol and biogas production: a review. Int J Mol Sci 9:1621–1651
13. Zhang K, Pei Z, Wang D (2016) Organic solvent pretreatment of lignocellulosic biomass for biofuels and biochemicals: a review. Bioresour Technol 199:21–33
14. Mou H, Wu S (2016) Comparison of organosolv and hydrotropic pretreatments of eucalyptus for enhancing enzymatic saccharification. Bioresour Technol 220:637–640
15. Bhutto AW, Qureshi K, Harijan K, Abro R, Abbas T, Bazmi AA, Karim S, Yu G (2017) Insight into progress in pre-treatment of lignocellulosic biomass. Energy 122:724–745
16. Lee SH, Doherty TV, Linhardt RJ, Dordick JS (2009) Ionic liquid-mediated selective extraction of lignin from wood leading to enhanced enzymatic cellulose hydrolysis. Biotechnol Bioeng 102:1368–1376
17. Shill K, Padmanabhan S, Xin Q, Prausnitz JM, Clark DS, Blanch HW (2011) Ionic liquid pretreatment of cellulosic biomass: enzymatic hydrolysis and ionic liquid recycle. Biotechnol Bioeng 108:511–520
18. Brandt A, Gräsvik J, Hallett JP, Welton T (2013) Deconstruction of lignocellulosic biomass with ionic liquids. Green Chem 15:550–583
19. Mäki-Arvela P, Anugwom I, Virtanen P, Sjöholm R, Mikkola JP (2010) Dissolution of lignocellulosic materials and its constituents using ionic liquids-a review. Ind Crop Prod 32:175–201
20. Da Costa Lopes AM, João KG, Bogel-ŁUkasik E et al (2013) Pretreatment and fractionation of wheat straw using various ionic liquids. J Agric Food Chem 61:7874–7882
21. George A, Brandt A, Tran K, Zahari SMSNS, Klein-Marcuschamer D, Sun N, Sathitsuksanoh N, Shi J, Stavila V, Parthasarathi R, Singh S, Holmes BM, Welton T, Simmons BA, Hallett JP (2015) Design of low-cost ionic liquids for lignocellulosic biomass pretreatment. Green Chem 17:1728–1734
22. Zhang Q, Hu J, Lee DJ (2017) Pretreatment of biomass using ionic liquids: research updates. Renew Energy 111:77–84
23. Wang F-L, Li S, Sun Y-X, Han HY, Zhang BX, Hu BZ, Gao YF, Hu XM (2017) Ionic liquids as efficient pretreatment solvents for lignocellulosic biomass. RSC Adv 7:47990–47998
24. Shen Y, Sun JK, Yi YX, Wang B, Xu F, Sun RC (2015) One-pot synthesis of levulinic acid from cellulose in ionic liquids. Bioresour Technol 192:812–816
25. Da Costa Lopes AM, Łukasik RM (2018) Separation and recovery of a hemicellulose-derived sugar produced from the hydrolysis of biomass by an acidic ionic liquid. ChemSusChem 11:1099–1107
26. Da Costa Lopes AM, Lins RMG, Rebelo RA, Łukasik RM (2018) Biorefinery approach for lignocellulosic biomass valorisation with an acidic ionic liquid. Green Chem 20:4043–4057
27. Hui W, Zhou Y, Dong Y, et al (2019) Efficient hydrolysis of hemicellulose to furfural by novel superacid SO4H-functionalized ionic liquids. Green Energy Environ 4:49–55
28. Prado R, Erdocia X, Labidi J (2016) Study of the influence of reutilization ionic liquid on lignin extraction. J Clean Prod 111:125–132
29. Ye C, Liu W, Chen Y et al (2001) Room-temperature ionic liquids: a novel versatile lubricant. Chem Commun 35:2244–2245
30. Forsyth SA, Pringle JM, MacFarlane DR (2004) Ionic liquids—an overview. Aust J Chem 57:113
31. Li C, Cheng G, Balan V, Kent MS, Ong M, Chundawat SPS, Sousa LC, Melnichenko YB, Dale BE, Simmons BA, Singh S (2011) Influence of physico-chemical changes on enzymatic digestibility of ionic liquid and AFEX pretreated corn Stover. Bioresour Technol 102:6928–6936

32. Li H-Y, Chen X, Wang C-Z, Sun SN, Sun RC (2016) Evaluation of the two-step treatment with ionic liquids and alkali for enhancing enzymatic hydrolysis of eucalyptus: chemical and anatomical changes. Biotechnol Biofuels 9:166
33. Mohtar S, Tengku Malim Busu T, Md Noor A et al (2015) Extraction and characterization of lignin from oil palm biomass via ionic liquid dissolution and non-toxic aluminium potassium sulfate dodecahydrate precipitation processes. Bioresour Technol 192:212–218
34. Chang K, Lin H, Chen P (2009) The optimal performance estimation for an unknown PEMFC based on the Taguchi method and a generic numerical PEMFC model. Int J Hydrog Energy 34:1990–1998
35. Kumar R, Mago G, Balan V, Wyman CE (2009) Physical and chemical characterizations of corn stover and poplar solids resulting from leading pretreatment technologies. Bioresour Technol 100: 3948–3962
36. Li C, Sun L, Simmons BA, Singh S (2013) Comparing the recalcitrance of Eucalyptus, pine, and switchgrass using ionic liquid and dilute acid pretreatments. BioEnergy Res 6:14–23
37. Li C, Tanjore D, He W, Wong J, Gardner JL, Thompson VS, Yancey NA, Sale KL, Simmons BA, Singh S (2015) Scale-up of ionic liquid-based fractionation of single and mixed feedstocks. BioEnergy Res 8:982–991
38. Sun N, Rahman M, Qin Y, Maxim ML, Rodríguez H, Rogers RD (2009) Complete dissolution and partial delignification of wood in the ionic liquid 1-ethyl-3-methylimidazolium acetate. Green Chem 11:646–655
39. Wildschut J, Smit AT, Reith JH, Huijgen WJ (2013) Ethanol-based organosolv fractionation of wheat straw for the production of lignin and enzymatically digestible cellulose. Bioresour Technol 135:58–66
40. Segal L, Creely JJ, Martin AE, Conrad CM (1959) An empirical method for estimating the degree of crystallinity of native cellulose using the X-ray diffractometer. Text Res J 29:786–794
41. Sun L, Li C, Xue Z, Simmons BA, Singh S (2013) Unveiling high-resolution, tissue specific dynamic changes in corn stover during ionic liquid pretreatment. RSC Adv 3:2017–2027
42. Kilpeläinen I, Xie H, King A, Granstrom M, Heikkinen S, Argyropoulos DS (2007) Dissolution of wood in ionic liquids. J Agric Food Chem 55:9142–9148
43. Yan B, Li K, Wei L, Ma Y, Shao G, Zhao D, Wan W, Song L (2015) Understanding lignin treatment in dialkylimidazolium-based ionic liquid-water mixtures. Bioresour Technol 196:509–517
44. Zhang S, Wang J, Lu X, Zhou Q (2014) Structures and interactions of ionic liquids. Springer, London
45. Doherty TV, Mora-Pale M, Foley SE, Linhardt RJ, Dordick JS (2010) Ionic liquid solvent properties as predictors of lignocellulose pretreatment efficacy. Green Chem 12:1967–1975
46. Heggset EB, Syverud K, Øyaas K (2016) Novel pretreatment pathways for dissolution of lignocellulosic biomass based on ionic liquid and low temperature alkaline treatment. Biomass Bioenergy 93: 194–200
47. Li W, Sun N, Stoner B, Jiang X, Lu X, Rogers RD (2011) Rapid dissolution of lignocellulosic biomass in ionic liquids using temperatures above the glass transition of lignin. Green Chem 13:2038
48. Brandt A, Hallett JP, Leak DJ, Murphy RJ, Welton T (2010) The effect of the ionic liquid anion in the pretreatment of pine wood chips. Green Chem 12:672–679
49. Passos H, Dinis TB, Cláudio AFM et al (2018) Hydrogen bond basicity of ionic liquids and molar entropy of hydration of salts as major descriptors in the formation of aqueous biphasic systems. Phys Chem Chem Phys 20:14234–14241
50. Kosan B, Michels C, Meister F (2008) Dissolution and forming of cellulose with ionic liquids. Cellulose 15:59–66
51. Brandt-Talbot A, Gschwend FJV, Fennell PS, Lammens TM, Tan B, Weale J, Hallett JP (2017) An economically viable ionic liquid for the fractionation of lignocellulosic biomass. Green Chem 19: 3078–3102
52. Shi J, Thompson VS, Yancey NA, Stavila V, Simmons BA, Singh S (2013) Impact of mixed feedstocks and feedstock densification on ionic liquid pretreatment efficiency. Biofuels 4:63–72
53. Raj T, Gaur R, Dixit P, Gupta RP, Kagdiyal V, Kumar R, Tuli DK (2016) Ionic liquid pretreatment of biomass for sugars production: driving factors with a plausible mechanism for higher enzymatic digestibility. Carbohydr Polym 149:369–381
54. Kim H, Ahn Y, Kwak SY (2016) Comparing the influence of acetate and chloride anions on the structure of ionic liquid pretreated lignocellulosic biomass. Biomass Bioenergy 93:243–253
55. Uju SY, Nakamoto A et al (2012) Short time ionic liquids pretreatment on lignocellulosic biomass to enhance enzymatic saccharification. Bioresour Technol 103:446–452
56. Leclerc DF (2006) Spectroscopy in the pulp and paper industry. In: Meyers RA (ed) Encyclopedia of analytical chemistry: applications, theory and instrumentation. Wiley, Chichester, pp 8361–8388
57. Li C, Knierim B, Manisseri C, Arora R, Scheller HV, Auer M, Vogel KP, Simmons BA, Singh S (2010) Comparison of dilute acid and ionic liquid pretreatment of switchgrass: biomass recalcitrance, delignification and enzymatic saccharification. Bioresour Technol 101:4900–4906
58. Liu D, Yu Y, Wu H (2013) Differences in water-soluble intermediates from slow pyrolysis of amorphous and crystalline cellulose. Energy Fuel 27:1371–1380
59. Perez-Pimienta JA, Lopez-Ortega MG, Chavez-Carvayar JA, Varanasi P, Stavila V, Cheng G, Singh S, Simmons BA (2015) Characterization of agave bagasse as a function of ionic liquid pretreatment. Biomass Bioenergy 75:180–188
60. Chen L, Sharifzadeh M, Mac Dowell N, Welton T, Shah N, Hallett JP (2014) Inexpensive ionic liquids: [HSO4]− based solvent production at bulk scale. Green Chem 16:3098–3106
61. Financie R, Moniruzzaman M, Uemura Y (2016) Enhanced enzymatic delignification of oil palm biomass with ionic liquid pretreatment. Biochem Eng J 110:1–7
62. Dibble DC, Li C, Sun L, George A, Cheng A, Çetinkol ÖP, Benke P, Holmes BM, Singh S, Simmons BA (2011) A facile method for the recovery of ionic liquid and lignin from biomass pretreatment. Green Chem 13:3255
63. Sun J, Shi J, Konda NVSNM et al (2017) Efficient dehydration and recovery of ionic liquid after lignocellulosic processing using pervaporation. Biotechnol Biofuels:1–14
64. Mai NL, Ahn K, Koo Y (2014) Methods for recovery of ionic liquids—A review. Process Biochem 49:872–881
65. Liang X, Fu Y, Chang J (2017) Research on the quick and efficient recovery of 1-allyl-3-methylimidazolium chloride after biomass pretreatment with ionic liquid-aqueous alcohol system. Bioresour Technol 245:760–767
66. Hou XD, Smith TJ, Li N, Zong MH (2012) Novel renewable ionic liquids as highly effective solvents for pretreatment of rice straw biomass by selective removal of lignin. Biotechnol Bioeng 109: 2484–2493
67. Chang H-C, Jiang J-C, Chen T-Y, Wang HS, Li LY, Hung WW, Lin SH (2013) Specific interactions between the quaternary ammonium oligoether-based ionic liquid and water as a function of pressure. Phys Chem Chem Phys 15:12734–12741
68. Chang H-C, Hsu D-T (2017) Interactions of ionic liquids and surfaces of graphene related nanoparticles under high pressures. Phys Chem Chem Phys 19:12269–12275
69. Chang H-C, Zhang R-L, Hsu D-T (2015) The effect of pressure on cation-cellulose interactions in cellulose/ionic liquid mixtures. Phys Chem Chem Phys 17:27573–27578

70. Chang H-C, Chang S-C, Hung T-C, Jiang JC, Kuo JL, Lin SH (2011) A high-pressure study of the effects of TiO 2 nanoparticles on the structural organization of ionic liquids. J Phys Chem C 115: 23778–23783
71. Tan X, Li X, Chen L, Xie F (2016) Solubility of starch and microcrystalline cellulose in 1-ethyl-3-methylimidazolium acetate ionic liquid and solution rheological properties. Phys Chem Chem Phys 18:27584–27593
72. Cummings J, Tremain P, Shah K, Heldt E, Moghtaderi B, Atkin R, Kundu S, Vuthaluru H (2017) Modification of lignites via low temperature ionic liquid treatment. Fuel Process Technol 155:51–58